Technology and Science for the Ships of the Future
V. Crupi and V. Bucci (Eds.)

doi:10.3233/PMST250032

Analysis of the Virtual Towing Tank Accuracy by Means of a New EFD Database

Simone BOZZO[a,b,1], Marco FERRANDO[c], Diego VILLA[d]
[a]*CSSN, Naval Support and Experimentation Centre, Italian Navy, Viale S. Bartolomeo 400, 19020 La Spezia,*
[b,c,d]*DITEN, Dipartimento di Ingegneria Navale, Elettrica, Elettronica e delle Telecomunicazioni, Università degli Studi di Genova, 16145 Genova, Italy,*
ORCiD ID: Simone BOZZO https://orcid.org/0009-0009-0470-6522
Diego VILLA https://orcid.org/0000-0001-6332-705X
Marco FERRANDO https://orcid.org/0000-0001-9131-5195

Abstract. This work introduces to the field of comparisons between the Experimental Fluid Dynamics (EFD) and Computational Fluid Dynamics (CFD). The ship resistance prediction can be, nowadays, performed by CFD techniques, but the accuracy of the result obtained is not still well identified. The notable absence of an extensive and freely accessible database, where both ships geometry and experimental data are available, induced the scientific community to organize workshops to investigate both the field of Verification and, most importantly, of the Validation (commonly named: V&V). In this work, through the use of an open-source viscous based code (i.e. OpenFOAMv8), and the availability of a significant experimental database, it has been tested a well-consolidated procedure to perform CFD calculations, with the aim to seed a comparative EFD vs. CFD repository which consists of about one-hundred simulations performed for fifteen different hull shapes. The generated repository has been analysed, in order to extract statistical considerations and assess potential correlations between the differences (among CFD calculations and EFD results) and other physical parameters. The main output of this analysis consists in having defined a mean absolute difference between physical and virtual towing tank tests of 3.2% with a standard deviation of 2.17%.

Keywords. EFD, CFD, towing tank test, V&V, uncertainty.

1. Introduction

In the second half of the 19th century, engine-driven propulsion systems started to replace sails and by that time all the projects concerning the design of a new ship aimed at defining if that ship was compliant or not with shipowner's requirements (i.e. speed requirements).

In 1868, William Froude proposed a new way to assess if the new design would perform as request. He "first recognized the practical necessity of separating the total resistance into components, based on the general law of mechanical similitude, from observation of the wave patterns of models of the same form but of different sizes" [1]. Based on this assumption, the marine towing tanks facilities started to grow alongside

[1] Corresponding Author: S. BOZZO, simone.bozzo@marina.difesa.it and simone.bozzo@edu.unige.it.

the newly conceived discipline which is nowadays known as Experimental Fluid Dynamic (EFD).

The "International Hydro-mechanical Congress" held in Hamburg in 1932 [2], established the groundwork for the development of a robust, constantly updated, freely accessible procedure drafted by the scientific committee, which nowadays can be found among the "International Towing Tank Conference" (ITTC) "Recommended Procedures and Guidelines", able to quantify the differences between experiments and reality with a reasonable level of reliability.

Meanwhile, a new type of technology was developing. Starting with the first generation of electronic digital computer, dated back in 1937 [3], the opportunity to solve numerically partial differential equations became an attainable result and so it can be recognized the birth of the Computational Fluid Dynamics (CFD) in that period of time.

With the first international workshop on the numerical prediction about viscous flow around ships, held in Gothenburg 1980, the phase of comparison between the results of tests and CFD calculations had begun. Ten years after this workshop, which can be considered a milestone in the field of CFD ship resistance, other conferences have taken place [4]. Looking at the number of benchmarks it is possible to assess that the comparison performed is only between three kind of hulls and many kinds of CFD codes. Within the scientific community, other works investigating the differences between EFD results and CFD calculations can be listed [5], [6]; thus, in these cases as well, the performed comparisons deal with a few hull or few speeds only.

The aim of this work, instead, deal with the assessment of the differences between the experimental measurements and the numerical predictions, for several hull shapes, performed using a numerical setup in-house developed and based on the open-source OpenFOAM environment. This activity could provide a different point of view on the numerical uncertainty with respect to the classical approaches present in literature.

2. The available experimental database

At the University of Genova, a collection of old volumes containing more than 200 experimental tests has been found. The experimental tests, performed mainly in La Spezia towing tank and in old Roma towing tank, are taken into account like benchmarks for CFD calculations. The hull shapes have been chosen carefully to gain an heterogenous family of data to be used for validating the CFD. Even if this database collects mainly old fashion hull shapes, its amount of data can be considered a valuable opportunity to test the CFD ability in the ship resistance predictions. In accordance with the ITTC Symbols and Terminology List [7], the principal data of considered model are summarized in Table 1.

Table 1. Main characteristics of the available database.

Dimension	Symbol	Minimum Value	Maximum Value	UoM
Length of waterline	L_{WL}	3.780	5.720	m
Maximum moulded breadth at design WL	B_{WL}	0.651	0.840	m
Draught at midship	T_M	0.185	0.327	m
Displacement volume	∇	0.231	0.848	m^3
Area of wetted surface	S	2.630	5.399	m^2
Area of maximum transverse section	A_X	0.183	0.204	m^2
Area of waterplane	A_W	2.638	3.241	m^2
Ratio L/B	L_{WL}/B_{WL}	5.053	7.628	-

Ratio B/T	B_{WL}/T_M	2.410	4.043	-
Block coefficient	$C_B = \nabla/LBT$	0.401	0.699	-
Scale ratio	$\lambda = L_s/L_M$	5.0	28.9	-
Froude number	$F_r = V/\sqrt{gL}$	0.05	0.416	-

3. Workflow description and numerical methodology

The procedure to use this repository, where both experimental results and CFD calculation will be stored, is described in detail in this paragraph.

3.1. Hull identification

The criteria used to select the EFD experiments to be reproduced numerically is connected with the parameters reported in Table 2. Each parameter has been selected to get a sufficiently heterogeneous range of values for the experimental data to look for correlation analysis between the EFD experiments and the CFD calculations. This should provide an adequately diversified measurements to perform the comparisons.

Table 2. Changes in the parameters considered in the selected EFD experiments**.**

Parameters	**Symbol**	**Value Ratio**		**UoM**
		Min	**Max**	
Model length	L_{WL}	3.780	5.720	[m]
Ratio L_{WL}/B	L_{WL}/B_{WL}	5.053	7.6283	[adim]
Ratio B/T	B_{WL}/T_M	2.410	4.0432	[adim]
Scale factor	$\lambda = L_s/L_M$	5.000	28.921	[adim]
Ship speed	$F_r = V/\sqrt{gL_{WL}}$	0.150	0.416	[adim]

3.2. 3-D model generation

Once the case has been selected, it is possible to generate the 3D digital twin of the hull to be tested. Beginning with the lines plan of the selected model, a 3D model of the hull (an example is illustrated in Figure 1) has been created (using FREE!ship, version 3.13+) and, the obtained CAD model has been subjected to a first verification, which consist of two checks:

- displacement volume check: based on $1-\left(\nabla_{M_{CFD}}/\nabla_{M_{EFD}}\right)$ formulation, the volume difference should be lower than 0.5%.
- test on hull form geometries: a consistency check between the given data and the 3D geometry (such as the area of water plane, its centre of flotation, the position of centre of buoyancy, the wetted surface area and hydrodynamical coefficients) is conducted, the overall difference must remain below 1%.

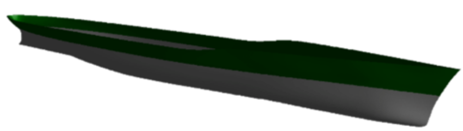

Figure 1. 3D model of the hull generated from the lines drawing.

Considering that the maximum Froude's number among the repository is close to 0.41 and all the hull tested are in displacement mode, these differences have a limited impact on the total resistance of the vessel; therefore, the proposed checks have been considered robust enough to get the 3D digital twin of the hull. While, considering a planning hull mode regime, the differences can affect the resistance [8], so they have to be taken into account.

3.3. Numerical approach

The open-source code OpenFOAM libraries (version 8) have been used to create a customized numerical setup applied to all the selected geometries.
The flow arising from the hull and any of its attached appendages can be sufficiently described by the Reynolds-averaged approach, in which the Navier-Stokes equations [9] are treated as reported in (1):

$$\begin{cases} \nabla \cdot \bar{\boldsymbol{u}} = 0 \\ \rho \frac{\partial \bar{\boldsymbol{u}}}{\partial t} + \rho(\bar{\boldsymbol{u}} \cdot \nabla \bar{\boldsymbol{u}}) = \rho \boldsymbol{g} - \nabla \bar{p} + \mu \nabla^2 \bar{\boldsymbol{u}} + \boldsymbol{T}_R \end{cases} \tag{1}$$

where $\bar{\boldsymbol{u}}$ represent the average velocity, $\bar{p}$ the average pressure fields, ρ the fluid density, μ its dynamic viscosity and $\boldsymbol{T}_R$ the Reynolds stresses tensor. In order to get the tensor properly modelled, in particular near to the wall, where a boundary layer is present, the k-ω SST two equation turbulence model has been used.

A finite volume method with cell-centered variables has been applied to solve the equation (1). Because of the presence of the free-surface among water and air, the interFOAM solver was chosen to perform all the simulations for a two-phase flow, immiscible and isothermal fluids. The volume of fluid approach (VoF) has been selected to capture the interface effects, because of its capability in modelling flows interfaces [10] and in gaining an excellent compromise between accuracy and computational effort as previously demonstrate also for a fast twin screw propellers ship [11].

Because of a steady-state solution is expected, to speed-up the solution convergence, the quasi-steady approach named Local Time Step (LTS) has been selected among the OpenFOAM libraries [12]. This model gives the possibility to arrange the time step for each cell inside the computational domain, keeping it to the minimum value, in line with the limit imposed by the local Courant number, as shown in equation (2):

$$C = (u \cdot \Delta t / \Delta x) \le C_{max} \tag{2}$$

where u is the flow speed, Δt is the local time step and Δx is the characteristic dimension of the cell in the flow direction.

The reference frame has been fixed into the intersection of the aft perpendicular with the free surface, the shape of the computational domain has been chosen as a parallelepiped box and, by considering the symmetry of the hull shape and to reduce the computational effort, all computations are performed with a symmetry boundary condition at the ship center-plane.

Moreover, to better reproduce the physical conditions adopted during towing tank tests, the hull is free to sink and trim according to the physics of the problem.

3.4. Mesh generation

Based on [13], the generation of the mesh inside the computational domain has been generated using a combination of the two utilities named blockMesh and cfMesh, available inside the OpenFOAM suite. The faces of the domain, which is defined as a parallelepiped box, represent the boundary for the numerical calculation and their characteristics are listed on Table 3, considering the reference frame centered in the intersection of the aft perpendicular with the free surface.

Table 3. Domain shape and size.

Boundary	Position [m]	Type
Upstream	$X=2.67*L_{WL}$	Velocity inlet
Downstream	$X=-2.67*L_{WL}$	Pressure outlet
Side	$Y=4.09*L_{WL}$	Symmetry plane
Centre symmetry plane	Y=0	Symmetry plane
Bottom	$Z=-1.39*L_{WL}$	Symmetry plane
Top	$Z=0.53*L_{WL}$	Symmetry plane
Ship model (half hull)	-	Wall

Three different type of refinements are used to better describe the physics of the problem: the first one consists of an anisotropic refinement across all the free surface of the domain, the second one consists of 5 boxes across the position of the hull with a hierarchical decrease refinement (cell size length factor 2), and the last consists of two prisms with a isosceles triangles base across the free surface to better describe the wave patterns, as shown in Figure 2.a and Figure 2.b.

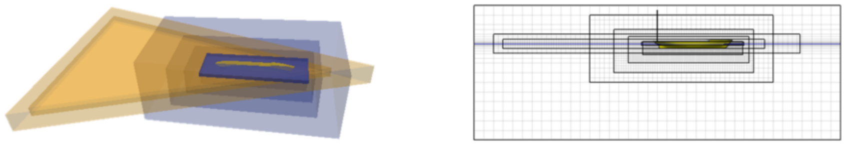

(a) (b)

Figure 2. 3-D view of the refinements (**a**) and sketch of the adopted mesh in the ship center-plane (**b**).

To account for the boundary layer development, each wall has its own prism layer region close to the wall itself; its thickness (BL) can be estimated trough the equation (3)

$$BL = \left(0.16 \cdot L/R_e^{(1/7)}\right)[m] \tag{3}$$

where L is the representative length of the wall considered and *Re* is the local Reynolds number.

The wall function approach has been utilized to describe the velocity profile close to the wall, and its thickness has been split accordingly with equation (4) to ensure that the y^+ value (non dimensional distance to the wall) remained below the reference value, fixed at 150.

$$y^+ = (y \cdot U/v)\ [adim] \tag{4}$$

The mesh generation operation has resulted in a mean value of cells for each simulation close to 2.2M cells.

3.5. Post processing analysis.

For each performed simulation, a post process analysis has been applied; in fact, after each simulation has finished, it was necessary to verify its numerical consistency. By looking at the history of the signal of the total resistance (R_T), it is possible to assess if the simulation has reached a convergence; in Figure 3.a a properly convergence simulation is shown where the mean value of the signal is calculated on the last 5000 iterations.

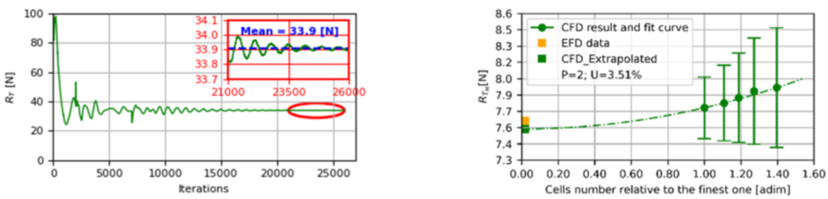

(a) (b)

Figure 3. History of the resistance signal (R_T) for an hull of the repository (**a**) and uncertainty analysis performed for the same hull at fixed speed with 5 different meshes respectively with 0.63M, 0.84, 1.03, 1.27 and 1.73 million cells (**b**).

Even though the uncertainty data for the EFD results aren't available, and therefore, in principle, it is not possible to achieve a full validation for the simulations performed as request by the ITTC's Recommended Procedure and Guidelines for CFD [14], the uncertainty analysis was carried out at the verification level for some hull. An example of the uncertainty analysis performed for one hull of the database (at the design speed) with five different meshes has been reported in Figure 3.b. The uncertainty quantification (UQ), firstly proposed by Eça - Hoekstra [15], has been here reported, showing a quite low uncertainty quantification of about 3.5% for the fine mesh.

For each simulation, ship and speed, all data coming out from the post-processing analysis are named and stored inside a repository into a standardized template to facilitate subsequent analyses.

4. The comparison repository

Applying the previous described procedure for different hulls, the repository has been generated. The database consists of 92 simulations for 15 types of ships at different speeds, coming from the available experimental database. For each performed simulation, it is possible to compare the obtained result with the experimental data by applying criterion $\Delta R_T = \left[\left(R_{T_{CFD}}/R_{T_{EFD}}\right) - 1\right]$ and reporting the difference, named "ΔR_T", as a percentage.

Different kinds of analyses can be carried out using the obtained data. Examining the ΔR_T value, it is possible, firstly, to perform a statistical-based analysis of the raw data, secondly to correlate the ΔR_T value with the geometry of the hulls or with the configuration of the test (bare/fully appended hull), and lastly looking for correlations among the value and the hydrodynamic main parameter.

4.1. Statistical-based analysis

As reported in Figure 4, where each point represents a single test for a generic hull at a generic speed, the average differences between the CFD calculations and the EFD results has been analyzed as a function of the non-dimensional ship speed (i.e. Froud number), considering or not its sign (Figure 4.a and Figure 4.b respectively). It is evident that the differences are reasonably balanced between underestimations ($\Delta R_T < 0$) and over-estimations ($\Delta R_T > 0$), in fact an average of 0.4% can be seen. Even if the standard deviation is less than 4%, some of them are in the range between 6 and 8% (except for an outlier where an error close to 10% is recorded). When the absolute differences are considered, the average value becomes only 3.24% with a standard deviation of 2.17%.

Consequently, for a blind calculation, it is possible to assess a mean difference between data and the calculation itself lower than 4% without any characterizations about its sign.

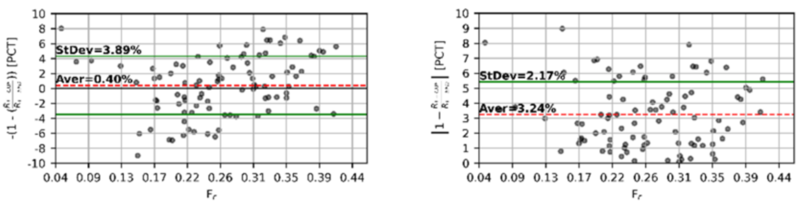

(a) (b)

Figure 4. Differences between CFD calculations and EFD results plotted as a function of the speed; differences with sign (**a**), absolute value of the difference (**b**).

The data can be further analyzed using the data discrete binning method; in fact, by splitting all the speed range in bins, it is possible to evaluate the mean value of the results inside that range. The speed range has been divided into 12 bins and the mean value was calculated for each bin, establishing consistency by setting a minimum of 5 samples per bin. As shown in Figure 5.a by the dash-dot red line with squares, a dependency of the difference with the speed is present and this difference tends to shift from an underestimated value to an over-estimated one increasing the ship speed.

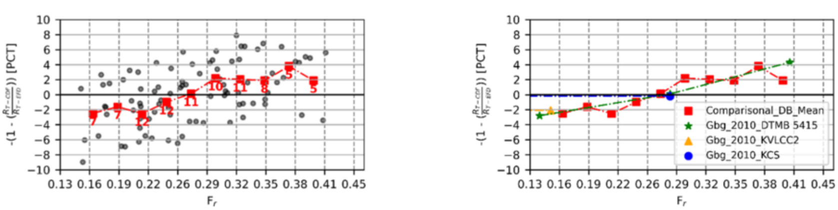

(a) (b)

Figure 5. Trend of differences between CFD calculations and EFD results plotted against velocity (obtained by splitting the speed range in bins and calculating for each one of them the local mean). Square represent the mean value of the bin, each number next to the square represents the number of occurrences inside that range (**a**). Trend of differences between CFD calculations and EFD results plotted against velocity with Gothenburg 2010 workshop 2010 results (**b**).

These results, where a single numerical set-up has been applied for all the cases tested, generally comply with the one reported by the Gothenburg 2010 workshop [4], where several codes and numerical set-ups performed the same simulations. In particular, as shown in Figure 5.b, considering the results for the DTMB 5415 hull in free trim condition (green line) results show a very good agreement among the differences with the one registered in the proposed database (red line). This is an important result which gives a consistency in the work performed; so, it is possible to move through further analysis of differences between the EFD results and the CFD calculations and consider these findings as indicative of an inherent consistency.

4.2. Differences versus hull geometry and configuration

To assess if correlations among results and geometrical characteristics are present, it is possible to divide the results as reported in Figure 5.a considering the presence or the absence of the appendages and the hull studied.

Each hull has been tested for different speeds to replicate the towing tank experience and for clarity of reading, each hull has an identification number and one color which identify always the same case in the current paper. The Figure 6, shows the data for each hull. Except for one case (identified as ID_15), for all the other results, the difference shows a trend with a positive rate of change when speed increase.

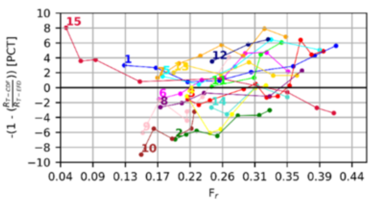

Figure 6. Trend of differences between CFD calculations and EFD results plotted against velocity (each case has an hull identification number and a different color).

Another way for interpreting the differences between CFD and EFD consists of looking at the configurations of the model tested; in particular it is possible to split the comparisons into two kinds of configurations: bare hull and fully appended.

Figure 7 reports, for each ship, the average error (square dots) and its standard deviation (upper and lower bars) between computations results and experimental data. From this figure, for the fully appended hulls the average standard deviation is equal to 2.77% (average between all the tests) while for the bare hull configuration it is equal to 2.02%. Except for few cases (like ID 15 where the model has been tested also in the very low-speed region where laminar phenomena may have taken place), in both configurations the standard deviation for each case is usually lower than the one obtained from the raw data analysis. This effect maybe be linked to the presence of a systematic error connected with the uncertainty deriving from the procedure to generate the 3D geometry starting from the available data (generally an image of the lines plan) and/or how the EFD data have been obtained (old procedures and old equipment for acquiring measurements). Hence, this kind of analysis leads to consider for a generic hull tested a mean difference with the experimental data in accordance with the one reported in 4.1 paragraph (3.24% with a standard deviation of 2.17%) but, if more confidence on the geometry and test conditions can be achieved, a lower uncertainty could be expected.

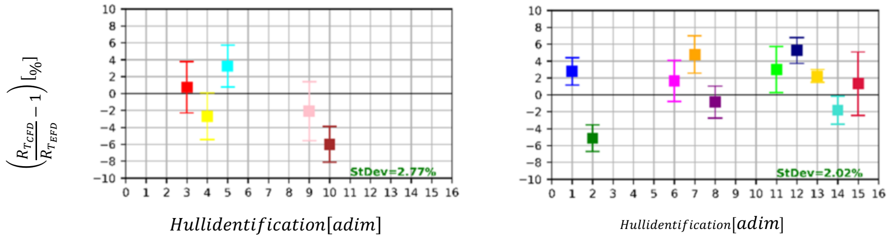

(a) with appendages (b) without appendages

Figure 7. differences between CFD calculations and EFD results plotted for each hull with appendages (**a**), and without appendages (**b**). The errors bars are representative of the mean value and its standard deviation of that hull.

4.3. Differences versus hydrodynamic main parameters and correlation analyses

An alternative approach to identify correlations in the results, is to compare them with the geometrical hull dimensions or coefficients of the models.

As stated by ITTC guidelines for the resistance test [16], the model should be as large as the dimensions of the tank allow and the onset of the blockage phenomenon should be prevented, a correlation analysis firstly considering the scale $\lambda = (L_{PP})_S/(L_{PP})_M$ of the model and secondly the length of the model $(L_{PP})_M$ has been carried out as shown in Figure 8.a and Figure 8.b respectively. Looking at the results obtained, nothing remarkable is revealed by this kind of analysis.

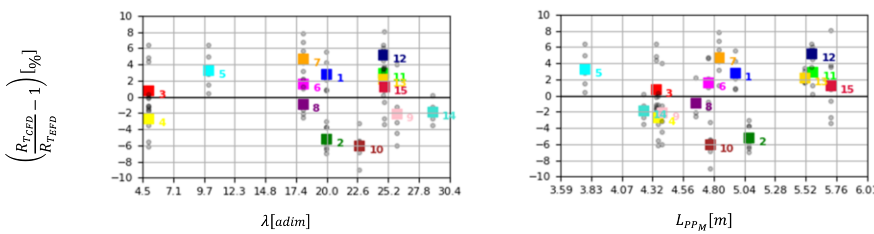

(a) (b)

Figure 8. Differences between CFD calculations and EFD results plotted against the scale ratio (**a**) and the length of the model (**b**) for all the cases studied.

The last comparison performed, as reported in Figure 9.a and Figure 9.b, deals with the main geometrical ratio L_{WL}/B_{WL} and B_{WL}/T respectively. Even upon conducting this last analysis, it remains impossible to draw a correlation between the geometrical ratios shown and the differences registered.

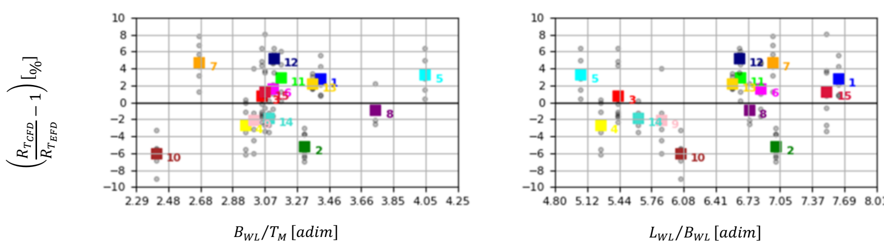

(a) (b)

Figure 9. Differences between CFD calculations and EFD results plotted against the ratio B_{WL}/T (**a**) and the ratio L_{WL}/B_{WL} (**b**) for all the cases studied.

5. Conclusions

A repository composed by 92 comparisons (for 15 different hulls) between the EFD results coming from the towing tank experiences and the CFD calculations has been presented in this article.

The created repository analysis has revealed that a general over on under estimation cannot be identified for the selected numerical set-up (an average difference of 0.4% is reported) between CFD calculations and EFD results for the total resistance of the models. Considering the differences, seen as the distance of the prediction by the measurements (differences without sign), the mean error consists of 3.24% with a standard deviation of 2.17%. So, it is possible to generalize the result described, considering an absolute mean difference between EFD and CFD of about 3.2%.

A weak but credible correlation was found between speed and differences such that at low speed, an under-estimation of CFD was recorded, while at high speed an overestimation of CFD prediction was observed. It is not possible to assess any clear correlation with the discrepancies and the hydrodynamic main parameters. Moreover, the presence of appendages in the models leads to a slightly higher standard deviation compared with the results coming from hulls tested without appendages. Thus, for each hull configuration is possible to assess that the standard deviation (seen as a sort of uncertainty of the prediction) is lower than the one obtained from the raw data and so, for a generic hull, the mean difference between EFD and CFD has a lower difference of about 2%. Differently a systematic gap is present for most of the considered models, ascribed to the uncertainty on the entire process to generate the simulation and if more confidence on the geometry and test conditions can be achieved, a lower uncertainty could be expected

This study paves the way for other kind of analysis in order to look for possible correlations between the accuracy of a CFD calculation and some physical issue and it requires other simulation to get a more extensive comparison database also including modern hull shapes where the geometries are properly described and ideally supported by the experimental uncertainty assessments to better reproduce the CFD ability with nowadays designs along with its level of uncertainty.

References

[1] Lewis EV. Principles of Naval Architecture: Resistance, Propulsion and Vibration 2nd ed. Jersey City: Society of Naval Architects and Marine Engineer; 1990. 5p, ISBN 0-939773-01-5.

[2] History of ITTC, from https://ittc.info/about-ittc/history/

[3] Zakari I, Yar U. History of computer and its generations. 2019.

[4] Larsson L, Stern F, Visonneau M. CFD in Ship Hydrodynamics—Results of the Gothenburg 2010 Workshop. In: MARINE 2011 - Computational Methods in Marine Engineering IV. 2013. p. 237–59, doi: 10.1007/978-94-007-6143-8_14.

[5] Islam H, Guedes Soares C. Uncertainty analysis in ship resistance prediction using OpenFOAM. Ocean Engineering. 2019 May 15; doi: 10.1016/j.oceaneng.2019.02.033.

[6] Villa D, Tani G, Gaggero S, Ferrando M, Ausonio P, Travi P, et al. A comprehensive analysis of a numerical self-propulsion procedure for high-speed marine vehicles. Ocean Engineering. 2023 Sep 11;287; doi: 10.2139/ssrn.4390637.

[7] International Towing Tank Conference, Symbols and Terminology List (Version 2021), from https://www.ittc.info/media/9882/alphabetic-ittc-symbols-list-2021.pdf.

[8] Lakatoš M, Mancini S, Niazmand B, Tabri K. Verification and validation of hard-chine hull performance in calm water: Effects of numerical setups and hull configurations. Ocean Engineering. 2025 Giu 15; 329; https://doi.org/10.1016/j.oceaneng.2025.121056.

[9] Gaggero S, Villa D, Viviani M. The Kriso container ship (KCS) test case: An open source overview. MARINE 2015 - Computational Methods in Marine Engineering VI. 2015 Jan 1;735–49.
[10] Wang Y, Rao H, Liu Z, Liu K, Zhou B, Zhang G. Numerical Prediction of Ship Resistance Based on Volume of Fluid Implicit Multi-Step Method. Journal of Marine Science and Engineering. 2023 Nov 16;11:2181; doi: 10.3390/jmse11112181.
[11] Bozzo S, Villa D. A Fast Numerical Procedure to Design the Shaftline Struts. In 2023. Doi: 10.3233/PMST230008.
[12] Yang X, An W, Li W, Zhang S. Implementation of a Local Time Stepping Algorithm and Its Acceleration Effect on Two-Dimensional Hydrodynamic Models. Water. 2020;12(4), doi: 10.3390/w12041148.
[13] Villa D, Furcas F, Pralits J, Vernengo G, Gaggero S. An Effective Mesh Deformation Approach for Hull Shape Design by Optimization. Journal of Marine Science and Engineering. 2021 Oct 12;9:1107. Doi: https://doi.org/10.3390/jmse9101107.
[14] International Towing Tank Conference, Uncertainty Analysis in CFD Verification and Validation Methodology and Procedures (7.5-03-01-01, approved 06/2021), https://www.ittc.info/media/9765/75-03-01-01.pdf
[15] Eça L, Hoekstra M. Evaluation of numerical error estimation based on grid refinement studies with the method of the manufactured solutions. Computers & Fluids. 2009 Sep 1;38:1580–91. Doi: 10.1016/j.compfluid.2009.01.003.
[16] International Towing Tank Conference, Resistance Tests (7.5-02-02-01, approved 06/2021), from https://www.ittc.info/media/9595/75-02-02-01.pdf